

Probing the physical properties of the NGC 5548 Broad Line Region using Balmer lines

Luka Č. POPOVIĆ,¹ Alla I. SHAPOVALOVA,² Vahram H. CHAVUSHYAN,³ Dragana ILIĆ,⁴ Alexandr N. BURENKOV,² Abelardo MERCADO⁵ and Nikolay G. BOCHKAREV⁶

¹*Astronomical Observatory, Volgina 7, 11160 Belgrade, Serbia*

lpopovic@aob.bg.ac.yu

²*Special Astrophysical Observatory of the Russian AS, Nizhnij Arkhiz, Karachaevo-Cherkesia 369167, Russia*

ashap@sao.ru

ban@sao.ru

³*Instituto Nacional de Astrofísica, Óptica y Electrónica, Apartado Postal 51, CP 72000, Puebla, Pue. México*

vahram@inaoep.mx

⁴*Department of Astronomy, Faculty of Mathematics, University of Belgrade, Studentski trg 16, 11000 Belgrade, Serbia*

dilic@matf.bg.ac.yu

⁵*Facultad de Ingeniería, Universidad Nacional Autónoma de Baja California, 21280, Mexicali, B.C., México*

abel@astroen.unam.mx

⁶*Sternberg Astronomical Institute, Moscow, Russia*

boch@sai.msu.ru

(Received 2007 July 15; accepted 2008 January 1)

Abstract

We investigate the physical characteristics of the Broad Line Region (BLR) of NGC 5548 using the Boltzmann plot (BP) method, that we applied on the Balmer lines observed from 1996 to 2004. We find that variability earlier detected in the lines, is also present in the temperature parameter A , obtained from the BP method. Using the BP temperature parameter A to calculate temperature, we find that the average temperature for the considered period was $T \approx 10000$ K, and that varies from 5000 K (in 2002) to 15000 K (in 1998). This variation correlates with the AGN-component of the optical continuum flux ($r = 0.85$) and may indicate the existence of an accretion disc in the BLR of NGC 5548.

Key words: galaxies: active – galaxies: individual: NGC 5548 – galaxies: Seyfert

1. Introduction

The physics and kinematics in the Broad Line Region (BLR) of Active Galactic Nuclei (AGN) is more complicated than in its Narrow Line Region (NLR) or in gaseous nebulae (Osterbrock 1989; Krolik 1999; Sulentic et al. 2000 and references therein). In contrast to the NLR where forbidden lines (e.g. [OIII] and [NII] lines) can be used as emitting plasma diagnostics, the physical conditions in the BLR cannot be obtained using simple relations between the line ratios. The pure recombination conditions cannot be applied in BLRs, e.g. the flux line ratios are different than expected in the case of recombination (e.g. in some AGN $Ly\alpha/H\beta \approx 10$, Osterbrock 1989).

Several effects can result in such line flux ratios of hydrogen lines, particularly the collisional excitation and extinction effects. For over more than 30 years now, numerous papers have been dedicated to this problem, see e.g. Netzer (1975), Ferland & Netzer (1979), Ferland et al. 1979, Kwan (1984), Rees et al. (1989), Ferland et al. (1992), Shields & Ferland (1993), Dumont et al. (1998), etc. Dust is present in the host galaxy of an AGN (see e.g. Crenshaw et al. 2002, Crenshaw et al. 2004, Gabel et al. 2005, etc.), but it seems that in some cases it can-

not explain the measured line flux ratios. The classical studies point toward photoionization, as the main heating source of the BLR emitting gas, that may explain observed spectra of AGN (see e.g. Kwan & Krolik 1981, Osterbrock 1989, Baldwin et al. 1995, Marziani et al. 1996, Baldwin et al. 1996, Ferland et al. 1998, Krolik 1999, Korista & Goad 2004). On the other hand, some authors e.g. Dumont et al. (1998) have given favor to a non radiatively heated region that contributes to the BLR line spectrum, which may be the case in the BLR of NGC 5548. Therefore, the photoionization, recombination and collisions could be considered as relevant processes that occur in BLRs. At larger ionization parameters, recombination is more important, but at higher temperatures or in the case of low ionization parameters the collisional excitation becomes important also (Osterbrock 1989). These two effects, as well as radiative-transfer effects in Balmer lines, should be taken into account when explaining the ratios of Hydrogen lines. Moreover, the geometry and possible stratification in the BLR may affect the continuum and line spectra of AGN (Goad et al. 1993).

Recently, Popović (2003, 2006ab) showed that in the BLR of some AGN, the Balmer line ratios follow the Boltzmann plot (BP), which indicates that the popula-

tion of the levels with $n \geq 3$ follow the Saha-Boltzmann equation. If the population of excited levels of the Balmer series can be described by Saha-Boltzmann equation, one can determine the temperature of the region where these lines are formed. This method, and also recently given method by Laor (2006) allow us to ascertain information about the physical (thermodynamical) properties of the BLR in a direct way by only measuring the broad line parameters (Ilić et al. 2007).

In order to test BP method as a tool for the temperature diagnostic in the BLR, we investigate here the spectra of NGC 5548 observed from 1996 to 2004 (Shapovalova et al. 2004). First, we found that BP method can be applied to the broad Balmer lines of NGC 5548, and after that we determined the temperature parameter A using the BP method.

NGC 5548 is one of the most intensively monitored Sy 1 galaxies (Shapovalova et al. 2004 and references therein) and the physics of its BLR have been studied by many authors (e.g. Krolik et al. 1991, Shields & Ferland 1993, O'Brien et al. 1994, Dumont et al. 1998, Vestergaard & Peterson 2005, Korista & Goad 2000, 2004). In particular, Dumont et al. (1998) discussed the physical model of the NGC 5548 BLR, and found inconsistencies between the photoionization model and the measured line fluxes, line flux variations and the underlying continuum. The aim of this work is to investigate the variations of the physical properties of the NGC 5548 BLR using the BP method and Balmer lines, during a period of 8 years.

2. The BP method

For plasma of the length ℓ that emits along the line of sight, the flux (or the spectrally integrated emission-line intensity) F_{ul} of the transition from upper to lower level ($u \rightarrow l$) can be calculated as (see also Popović 2006b):

$$F_{ul} = \frac{hc}{\lambda} g_u A_{ul} \int_0^\ell N_u(x) dx \quad (1)$$

where λ is transition wavelength, g_u statistical weight of the upper level, A_{ul} transition probability, N_u is the number density of emitters excited in upper level which effectively contribute to the line flux (which are not absorbed) and h and c are the well known constants (Planck and speed of light). In general, the N_u can be inhomogeneous across the line of sight and also, the radiative self-absorption can be present. But, assuming that population in the observed region (in all layers) follows the Saha-Boltzmann distribution one can write

$$N_u(x) \approx \frac{N_0(x)}{Z} \exp(-E_u/kT(x)), \quad (2)$$

where Z is the partition function, N_0 is the total number density of radiating species, E_u is the energy of the upper level, T is temperature and k is the Boltzmann constant.

In the case of optically thin plasma¹ with relatively

small changes in the density and temperature one can write (see, e.g., Griem 1997; Konjević 1999)

$$F_{ul} = \frac{hc}{\lambda} g_u A_{ul} \int_0^\ell N_u dx \approx \frac{hc}{\lambda} A_{ul} g_u \ell \frac{N_0}{Z} \exp(-E_u/kT). \quad (3)$$

For one line series (as e.g. Balmer line series) if the population of the upper energy states ($n \geq 3$)² adheres to a Saha-Boltzmann distribution than one can determine their temperature (T), from a Boltzmann plot as

$$\log(F_n) = \log \frac{F_{ul} \cdot \lambda}{g_u A_{ul}} = B - AE_u, \quad (4)$$

where F_n is normalized flux, B and A are BP parameters. Parameter A , defined as $A = \log_{10}(e)/kT$ (where $e \approx 2.718$), is the temperature indicator out of which we can estimate the temperature of the region where these lines are formed.

On the other hand, one cannot expect the homogeneous distribution of the physical parameters and density of emitters across the line of sight in an extensive BLR. But, if we still have that population follows the Saha-Boltzmann equation, Eq. (1) can be written as:

$$F_{ul} = \frac{hc}{\lambda} g_u A_{ul} \int_0^\ell \frac{N_0(x)}{Z} \exp(-E_u/kT(x)) dx \quad (5)$$

and if we divide the BLR in small layers with the same physical conditions and emitter density, then we can write:

$$F_{ul} = \frac{hc}{\lambda} g_u A_{ul} \sum_{i=1}^n \frac{N_0(i)}{Z} \exp(-E_u/kT(i)) \ell_i. \quad (6)$$

If we assume that the temperatures across the BLR vary as $T(i) = T_{av} \pm \Delta T_i$ and emitter density as $N_0(i) = N_0^{av} \pm \Delta N_0(i)$, the Eq. (6) can be written as:

$$I_{ul} = \frac{hc}{\lambda} g_u A_{ul} \frac{N_0^{av}}{Z} \sum_{i=1}^n (1 + \delta N_0(i)) \exp \left[-\frac{E_u}{kT_{av}(1 + \delta T_i)} \right] \ell_i, \quad (7)$$

where $\delta T_i = \Delta T_i/T_{av}$ and $\delta N_0 = \Delta N_0/N_0^{av}$. If in a BLR the temperature and emitter density does not vary too much, i.e. $\Delta N_0/N_0 \ll 1$ and $\Delta T_i/T_{av} \ll 1$, then the Eq. (7) becomes

$$I_{ul} = \frac{hc}{\lambda} g_u A_{ul} \frac{N_0^{av}}{Z} \exp(-E_u/kT_{av}) \ell. \quad (8)$$

meaning that the Eq. (4) can be used to determine T_{av} in the BLR (see Popović 2006b).

Radiative transfer issues (e.g. high optical depths of the Hydrogen lines) complicates the picture, but some additional tests are possible (see §5.2 and also Ilić 2007). Furthermore, the "Case B" recombination line ratios can produce similar Boltzmann plots of the Balmer line series in some AGN whose BLR is close to "Case B" recombination (see Osterbrock 1989). Due to the physical conditions (densities and temperatures) in such BLRs the constant A is too small ($A < 0.2$) and the Boltzmann plot cannot be applied for diagnostics of the temperature even if the

¹ Note here that we cannot expect that plasma in the BLR is optically thin, further in the text we will consider possible distribution of emitters within the BLR, see Eq. (5)

² Note here that since the emission deexcitation goes as $u \rightarrow l$ it is not necessary that level l has a Saha-Boltzmann distribution.

BP can be properly applied (Popović 2003, 2006ab, Ilić et al. 2006).

We should emphasize that the BP method (Popović 2003, 2006ab) does not take into account any *a priori* physics in the BLR, besides that the Balmer lines are originating in the same emitting region. The method includes the intensities and transition parameters of five Balmer lines, not only the ratio of two or three lines, as usually considered. We would like to point out that the BP is not the Balmer decrement, i.e. the ratio of the Balmer lines. Also, with this method, we concentrate on the thermodynamical state of the BLR trying to see if the BP method works at all, without assumptions on any "macroscopic" model caused by the "microscopic" physics.

3. Observations and selection of the spectra

Optical spectra of NGC 5548 were taken with the 6 m and 1 m telescopes of SAO (Russia, 1996-2004) and at INAOE's 2.1 m telescope at the Guillermo Haro Observatory (GHO) at Cananea, Sonora, Mexico (1998-2004). They were obtained with a long slit spectrograph equipped with CCDs. The typical wavelength range covered was from 4000 Å to 7500 Å, the spectral resolution was 4.5-15 Å, and the S/N ratio was >50 in the continuum near the H α and H β . Spectrophotometric standard stars were observed every night. Details concerning the spectroscopic observations are given in Shapovalova et al. (2004).

Note that the spectra of NGC 5548 were obtained under the AGN spectral monitoring program with the aim to study the variability of the broad Balmer emission lines H α and H β . The errors of the continuum at 5100Å and line fluxes were about 3-5%. From the spectral database collected during the monitoring program of NGC 5548 (≈ 150 spectra) we selected only 24 spectra (Table 1), which satisfy the following:

1. good photometric conditions;
2. S/N > 10 in the continuum near the H ϵ line;
3. spectrum covers the wavelength range from $\lambda 4000\text{Å}$ to $\lambda 7000\text{Å}$;
4. the broad component of the Balmer lines from H α to H ϵ are presented.

The basic data of these observations are presented in Table 1.

The spectrophotometric data reduction was carried out either with the software developed at the SAO RAS by Vlasyuk (1993) and with IRAF for the spectra obtained in Mexico. The image reduction process included bias subtraction, flat-field corrections, cosmic ray removal, 2D wavelength linearization, sky spectrum subtraction, stacking of the spectra for every set-up, and flux calibration based on standard star observations. We also remove the continuum of the host galaxy.

The procedure of absolute calibration of the spectra is described in details in Shapovalova et al. (2004) and will not be repeated here.

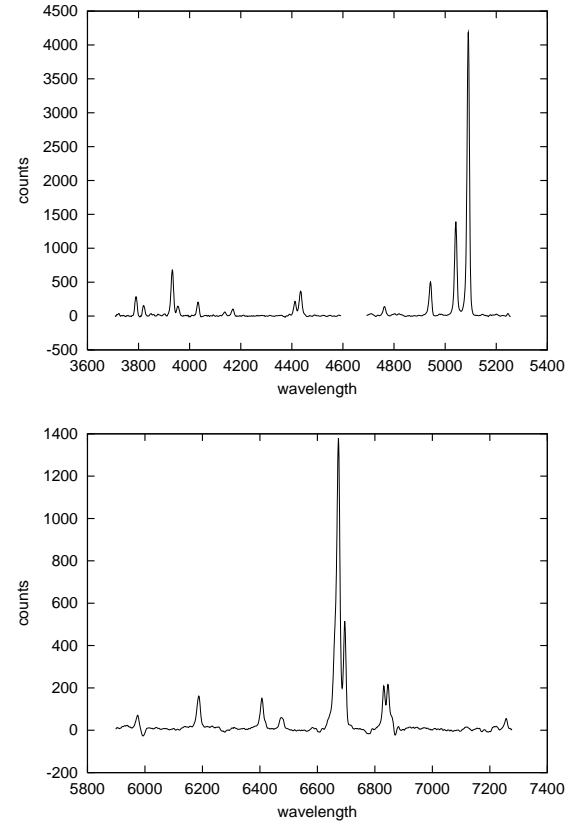


Fig. 1. The adopted narrow emission line template.

4. Measurements of the broad line flux

One can expect that the BP can be applied only in the case of the broad Balmer lines (Popović 2003), and first step was to subtract the continuum and the narrow and satellite lines from the Balmer lines. To estimate the contribution of these lines we used a template of narrow and satellite lines (Figure 1) estimated from two independent measurements in the case of the minimum intensity of the broad Balmer lines. In this template the Fe II lines in the H β spectral region are included. The optical Fe II lines showed variability with smaller amplitude than that of the H β (around 50%-75% of H β , Vestegaard & Peterson 2005). Testing the contribution of the Fe II residuals (after subtraction of the template), we concluded that it may contribute about 2-5% to the total measured line flux of the H β line.

Furthermore, we *a priori* take into account that the continuum subtraction contributes to the error-bars within 10% of the measured fluxes. In general, we can expect this value in weak Balmer lines (e.g. H ϵ), but in the case of the H α and H β lines, it should be even smaller.

The fluxes of the Balmer lines were measured several times, but it is important that independent measurements were performed by two persons. Then, the error-bars were calculated as:

$$\Delta F_i = \Delta F_i^{mes} + 0.1 \cdot F_i^{mes} \quad (9)$$

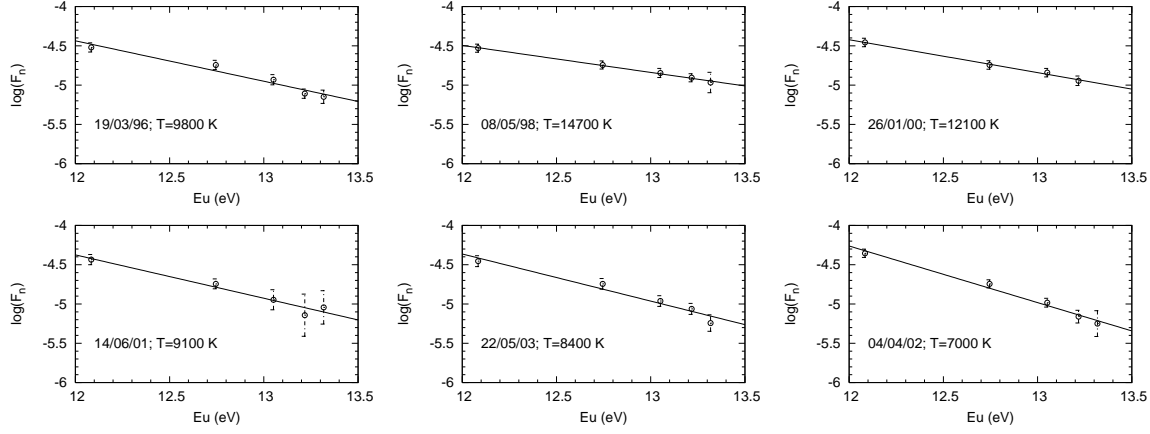


Fig. 2. The Boltzmann Plots of the Balmer line series of NGC 5548 from different periods. F_n is calculated using the Eq. (4) after the normalization of all Balmer lines to the $H\beta$ flux ($F_{ul}(H\beta) = 1$).

where F_i^{mes} is the measured flux, ΔF_i^{mes} is statistical error (within 1σ) obtained from several measurements and $0.1F_i^{mes}$ is taken to be the error of the continuum and narrow line template subtraction. The flux ratios of the Balmer lines and the fluxes of the $H\beta$ from different periods are given in Table 2. The error-bars presented in the Table 2 were obtained as (see e.g. Agekyan 1972, Bevington & Robinson 2003):

$$\Delta R_i = R_i \cdot \sqrt{\left(\frac{\Delta F_i}{F_i^{mes}}\right)^2 + \left(\frac{\Delta F_{H\beta}}{F_{H\beta}^{mes}}\right)^2} \quad (10)$$

where R_i is the ratio of $F_i/F_{H\beta}$.

In Figure 2 the error-bars ($\Delta \log_{10}(F_n)$) have been calculated as:

$$\Delta \log_{10}(F_n) = \frac{\Delta F_i}{F_i^{mes} \times \log_e 10}. \quad (11)$$

One can conclude from Eq. (4) that the absolute scale is not important for the BP analysis, which uses the slope to determine the temperature coefficients (A), but one should re-scale fluxes of Balmer lines for the same factor as well as the ΔF_i . The parameters A are obtained from the best fit of the measured values and we give asymptotic standard error ΔA (within 1σ) in Table 2.

We should note here that we used only those observed spectra where the spectral region from $H\epsilon$ to $H\alpha$ was covered, except for the two spectra (see Table 2) that covered only the interval from $H\delta$ to $H\alpha$. We used the aforementioned spectra in order to have the data in years 2000 and 2001.

4.1. Reddening

The reddening effect can influence the Balmer line ratio (e.g. Crenshaw & Kraemer 2001; Crenshaw et al. 2001; 2002; Popović 2003) and consequently the temperature parameter obtained by the BP. In the case of NGC 5548 the Galactic reddening is negligible $E(B-V) = 0.020$ mag (Burstein & Heiles 1982; Schlegel et al. 1998), and here it is not considered. Concerning the intrinsic reddening, in first approximation we can adopt that it might be 30% -

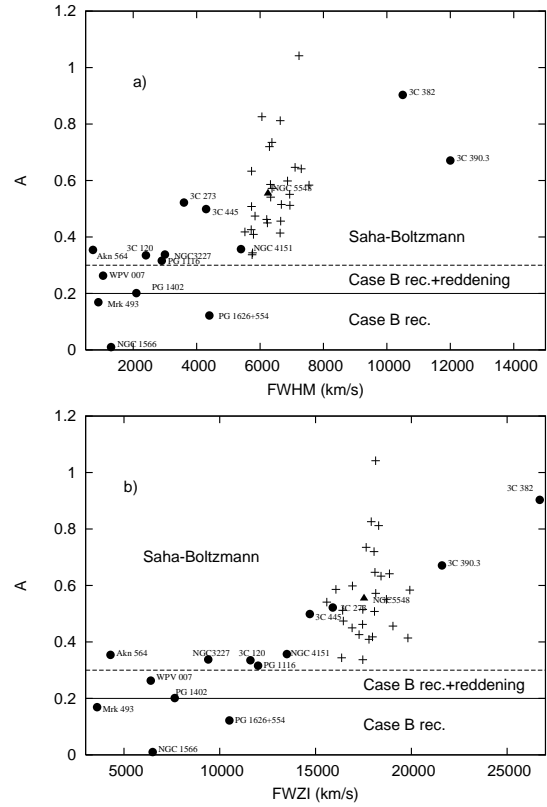


Fig. 3. The graph $A=f(\text{FWHM}, \text{FWZI})$. The data from different periods are denoted with crosses, while the averaged value for NGC 5548 is presented with full triangles. The data presented with full circles are taken from Popović (2003).

Table 1. The basic data of the spectroscopic observations of NGC 5548. The column "Code" refers to the telescope used for the observations: L - 6m telescope SAO RAS (Russia), GH - 2.1m telescope GHO (Cananea, Mexico).

| File (spectra) | UT-Date | JD (2400000+) | Code | Aperture (arcsec) | Sp.range (Å) | Resolution (Å) | Seeing (arcsec) |
|-------------------|-----------|------------------|------|----------------------|-----------------|-------------------|--------------------|
| 960213 | 1996Feb14 | 50127.579 | L | 1.5" x 6.0" | 3100-7200 | 6 | 2 |
| 960214 | 1996Feb14 | 50128.432 | L | 1.5" x 6.0" | 3100-7200 | 6 | 3 |
| 960319 | 1996Mar19 | 50162.382 | L | 2.0" x 6.0" | 3600-7400 | 8 | 3 |
| 960321 | 1996Mar21 | 50164.395 | L | 2.0" x 6.0" | 3600-7400 | 8 | 3 |
| 960710 | 1996Jul10 | 50275.283 | L | 2.0" x 6.0" | 3600-7000 | 8 | 1.4 |
| 980120 | 1998Jan21 | 50834.632 | L | 2.0" x 6.0" | 3800-7600 | 8 | 3 |
| 980222 | 1998Feb23 | 50867.535 | L | 2.0" x 6.0" | 3800-7600 | 8 | 2 |
| 980504 | 1998May04 | 50938.293 | L | 2.0" x 6.0" | 3700-7600 | 8 | 2.5 |
| 980508 | 1998May08 | 50942.461 | L | 2.0" x 6.0" | 3700-7700 | 8 | 2 |
| 980725 | 1998Jul26 | 51020.703 | GH | 2.5" x 6.0" | 3960-7231 | 15 | 2.2 |
| 980726 | 1998Jul27 | 51021.712 | GH | 2.5" x 6.0" | 3930-7219 | 15 | 2.5 |
| 200126 | 2000Jan27 | 51570.959 | GH | 2.5" x 6.0" | 4070-7350 | 15 | 2.5 |
| 210513 | 2001May14 | 52043.859 | GH | 2.5" x 6.0" | 3980-7300 | 15 | 1.8 |
| 210613 | 2001Jun14 | 52074.772 | GH | 2.5" x 6.0" | 4022-7330 | 15 | 1.8 |
| 210614 | 2001Jun15 | 52075.738 | GH | 2.5" x 6.0" | 4010-7330 | 15 | 1.8 |
| 21-07 | 2001Jul16 | 52107.320 | L | 2.0" x 6.0" | 3630-8050 | 8 | 2 |
| 220304 | 2002Mar05 | 52338.780 | GH | 2.5" x 6.0" | 3976-7305 | 15 | 2 |
| 220404 | 2002Apr05 | 52369.850 | GH | 2.5" x 6.0" | 3976-7305 | 15 | 2 |
| 220405 | 2002Apr06 | 52370.780 | GH | 2.5" x 6.0" | 3976-7305 | 15 | 2 |
| 220624 | 2002Jun24 | 52450.420 | L | 2.0" x 6.0" | 3800-7600 | 8 | 2 |
| 230126 | 2003Jan27 | 52666.96 | GH | 2.5" x 6.0" | 3976-7305 | 15 | 2.5 |
| 230127 | 2003Jan28 | 52667.930 | GH | 2.5" x 6.0" | 3976-7305 | 15 | 2.5 |
| 230325 | 2003Mar26 | 52724.900 | GH | 2.5" x 6.0" | 3976-7305 | 15 | 3.5 |
| 230522 | 2003May23 | 52782.750 | GH | 2.5" x 6.0" | 3976-7305 | 15 | 3.5 |

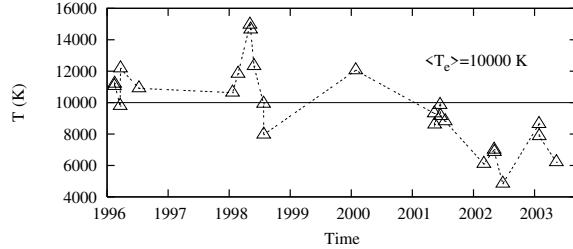


Fig. 4. The temperature variation from 1996 till 2004.

40%, as it was given in Popović (2003). But, since we are investigating the changes in the BP during an interval the intrinsic reddening can be neglected as it should not vary too much in a relatively short period of around 8 years.

4.2. Velocity Measurements

These measurements were performed in order to present A as a function of Full Width Half Maximum (FWHM) and Full Width Zero Intensity (FWZI). The graphs A vs. FWHM and FWZI are useful because of:

(i) the Balmer line ratios are velocity dependent in AGN (Stirpe 1990,1991) and this may be related to the physical conditions (temperature, density and kinematics) as well as to the radiative transfer effects;

(ii) illustration of the physical conditions in the BLR plasma. As it was pointed out by Popović (2003) if $A < 0.3$, the recombination "Case B" plus the intrinsic

reddening may explain BP. The "Case B" recombination of Balmer lines can bring the $\log(F_n)$ vs E_u as a linear decreasing function (see Table 4.4 in Osterbrock 1989).

In order to compare the temperature parameter A with the velocity of gas, very high data quality is required. The data quality is different for different spectra of NGC 5548. Consequently, for velocity measurements we used only the $H\alpha$ and $H\beta$ lines. We first normalized the broad profiles of these lines and converted the wavelength axis to the velocity scale $X = (\lambda - \lambda_0)/\lambda_0$ (the same as was given in Popović 2003). We measured FWHM and FWZI of both lines, and we calculated the average values for each spectrum.

5. Results and discussion

5.1. BP of NGC 5548

The results of our investigations are presented in Figures 2-4, and in Table 2.

One can see in Figures 2 and 3 that BPs graphics indicate that the population of the excited levels from the Balmer series follows the Saha-Boltzmann distribution. We found that in all considered periods, the temperature parameter is $A > 0.3$. It means that the recombination "Case B" plus an intrinsic reddening cannot explain the line flux ratio of the Balmer lines. Also, we investigate the dependence of the temperature coefficient as a function of FWHM and FWZI (Figure 3). As one can see from Figure 3, there is no significant correlation between

Table 2. The measured flux of the Balmer lines of NGC 5548, temperature parameter A .

| Spectra | $F_{H\alpha}/F_{H\beta}$ | $F_{H\gamma}/F_{H\beta}$ | $F_{H\delta}/F_{H\beta}$ | $F_{H\epsilon}/F_{H\beta}$ | $F_{H\beta}$ (erg · cm ⁻² s ⁻¹) | A |
|---------|--------------------------|--------------------------|--------------------------|----------------------------|--|-------------|
| 960213 | 3.405±0.406 | 0.396±0.047 | 0.174±0.021 | 0.071±0.027 | (7.998±0.950)E-13 | 0.456±0.095 |
| 960214 | 3.689±0.625 | 0.456±0.074 | 0.148±0.025 | 0.091±0.016 | (7.598±1.220)E-13 | 0.450±0.085 |
| 960319 | 3.647±0.492 | 0.341±0.051 | 0.133±0.018 | 0.077±0.015 | (7.281±0.983)E-13 | 0.515±0.068 |
| 960321 | 3.126±0.384 | 0.386±0.048 | 0.187±0.029 | 0.072±0.016 | (7.055±0.864)E-13 | 0.414±0.100 |
| 960710 | 4.203±0.569 | 0.465±0.063 | 0.204±0.027 | 0.084±0.011 | (9.891±1.322)E-13 | 0.462±0.082 |
| 980120 | 3.672±0.446 | 0.393±0.048 | 0.220±0.038 | 0.062±0.008 | (8.420±1.023)E-13 | 0.474±0.138 |
| 980222 | 3.624±0.429 | 0.376±0.072 | 0.210±0.027 | 0.082±0.023 | (9.694±1.146)E-13 | 0.426±0.075 |
| 980504 | 3.523±0.398 | 0.401±0.048 | 0.201±0.024 | 0.125±0.042 | (9.650±1.090)E-13 | 0.337±0.013 |
| 980508 | 3.571±0.427 | 0.416±0.055 | 0.212±0.025 | 0.117±0.035 | (7.998±0.950)E-13 | 0.344±0.014 |
| 980725 | 3.961±0.471 | 0.417±0.049 | 0.167±0.020 | 0.072±0.009 | (9.969±1.179)E-13 | 0.508±0.088 |
| 980726 | 3.727±0.438 | 0.338±0.047 | 0.153±0.018 | 0.039±0.012 | (9.235±1.083)E-13 | 0.633±0.177 |
| 200126 | 4.223±0.528 | 0.420±0.052 | 0.194±0.027 | - | (7.167±0.886)E-13 | 0.418±0.022 |
| 210513 | 5.718±1.134 | 0.314±0.099 | 0.109±0.049 | 0.146±0.096 | (2.900±0.437)E-13 | 0.586±0.161 |
| 210613 | 4.493±0.622 | 0.414±0.056 | 0.150±0.077 | - | (3.874±0.524)E-13 | 0.512±0.073 |
| 210614 | 4.439±0.664 | 0.330±0.097 | 0.123±0.076 | 0.098±0.048 | (3.408±0.499)E-13 | 0.551±0.070 |
| 21-07 | 4.028±0.521 | 0.390±0.065 | 0.166±0.024 | 0.055±0.009 | (5.901±0.749)E-13 | 0.572±0.127 |
| 220304 | 5.411±0.784 | 0.289±0.042 | 0.125±0.022 | 0.035±0.012 | (3.616±0.520)E-13 | 0.826±0.143 |
| 220404 | 5.347±0.654 | 0.303±0.039 | 0.118±0.022 | 0.061±0.023 | (7.998±0.950)E-13 | 0.720±0.049 |
| 220405 | 5.619±0.895 | 0.329±0.052 | 0.126±0.023 | 0.057±0.019 | (3.311±0.523)E-13 | 0.735±0.064 |
| 220624 | 4.781±1.127 | 0.057±0.017 | 0.062±0.011 | 0.029±0.012 | (2.691±0.472)E-13 | 1.042±0.276 |
| 230126 | 6.546±0.984 | 0.292±0.066 | 0.168±0.032 | 0.140±0.048 | (2.421±0.364)E-13 | 0.584±0.117 |
| 230127 | 6.794±1.176 | 0.208±0.040 | 0.162±0.030 | 0.130±0.032 | (2.136±0.369)E-13 | 0.641±0.167 |
| 230325 | 4.532±0.707 | 0.238±0.039 | 0.160±0.026 | 0.079±0.031 | (3.252±0.505)E-13 | 0.586±0.077 |
| 230522 | 4.248±0.677 | 0.318±0.050 | 0.148±0.024 | 0.062±0.015 | (4.782±0.758)E-13 | 0.599±0.073 |

widths and A . That is expected since macroscopic bulk motions are mainly constrained by kinematics, probably an accretion disc as it was suggested by Shapovalova et al. (2004). On the other hand, it may indicate that changes in the self-absorption in the Balmer lines has no significant variation during the period. The averaged value obtained from all periods (full triangle in Figure 3) is in good agreement with the trend of the AGN sample given in Popović (2003). Such a trend (increasing A with FWHM and FWZI) may indicate that physical conditions are dependent on kinematical characteristics of the BLR. This may be connected with distances from the massive black hole, e.g. the broader Balmer lines indicate higher macroscopic bulk motions which can be expected in the regions closer to the massive black hole.

Also, we could estimate the temperature using Eq. (3) & (4) from:

$$T \approx \frac{5060}{A} \text{ [K]}. \quad (12)$$

In Figure 4 we plotted the temperature variation in the considered period: as one can see the averaged temperature is ≈ 10000 K, and is changing by around 50% in the considered period. The maximum value of the temperature was reached in 1998 and minimum in 2002. The obtained temperatures agree well with the ones expected in the BLR.

On the other hand, from the BP fits, we obtained the parameter B . As it can be seen from Eqs. (1)-(4) the parameter B depends on the number density of radiating species and the partition function ($B = \log(hcN_0/Z)$).

Both values are the same for the Balmer line series at one moment, but they are changing during the time, since we expect that the physical properties in the emitting BLR plasma of NGC 5548 are changing (seen as variability in the broad spectral lines). In principle the partition function depends on the temperature and the level configuration (in our case Z is given for $n = 2$). It is hard to find some real information about variation in the number density in the BLR plasma using the B parameter, but still one can have impression about magnitude of variations of these two quantities. Taking into account Eqs. (1) - (4) and also the fact that we normalized Balmer line fluxes to the $H\beta$ flux, we can write $\log(N_0/Z) \sim B_{E_l} + \log(F_{H\beta})$ (h and c are constants, and B_l is intercept corresponding to the energy of the lower level, since Z is given for $n = 2$, $E_l = 10.2$ eV). Using this relation we found the difference between maximal and minimal value of $\log(N_0/Z)$ to be $\Delta \log(N_0/Z) = \log(N_0/Z)_{max} - \log(N_0/Z)_{min} \sim 0.9$. This can be expected, e.g. if we roughly approximate that Z stay constant, then maximal variation of number density is ~ 8 times, this is in an agreement with observed magnitude of variation in spectral lines of NGC 5548 (e.g. the flux of the $H\beta$ was changing ~ 5 times.)

5.2. Continuum vs. Temperature

Here we start from the fact that the response of the broad lines to continuum variations in NGC 5548 suggests that BLR is very close to the continuum source (Ferland et al. 1992), or it may even indicate that a part of optical continuum is originating in the BLR as well. We assume that the continuum is originating in an accretion

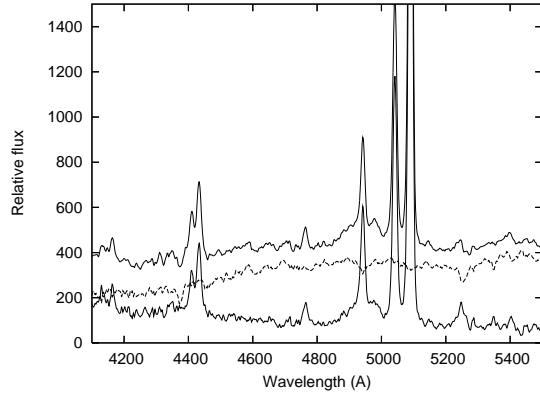


Fig. 5. The continuum flux of NGC 5548 in minimum before (top solid line) and after (bottom solid line) subtraction of the host galaxy continuum (dashed line).

disc, e.g. Kong et al. (2004) explained the variation in the optical spectral index with the variation in accretion parameters of the inner part of the disc. On the other hand, the Balmer lines may also be emitted from outer part of the accretion disc (Shapovalova et al. 2004), then the temperature variation measured from BP should be connected with the continuum variation. Therefore, we investigate the continuum intensity as a function of obtained temperatures. In an accretion disc, temperature depends on the radius (see e.g. Shakura & Sunyaev 1973) but if the continuum is emitted mostly from inner parts of the disc and Balmer lines mostly from outer parts, one can approximate that T_c correlates with the BLR temperature, i.e. $T_c \sim T_{BLR}$.

To find the correlation, we measured the flux in a window from 4240 Å to 4260 Å (rest-frame wavelengths) and calculated an average value for 4250 Å as well as in the spectral range from 5090 Å to 5110 Å (rest wavelengths) with an average value at 5100 Å.

In order to have only the AGN-component of the optical continuum, one should subtract the continuum of the host galaxy from the observed continuum of NGC 5548 nucleus. For this purpose, the contribution of the host galaxy at wavelengths 4250Å and 5100Å was obtained as following:

a) according to the paper by Romanishin et al. (1995, Fig. 5) the host galaxy contribution in the AGN continuum of NGC 5548 at 5100 Å in the aperture $5'' \times 7.5''$ is $F(5100) = (2.9 \pm 0.54) \cdot 10^{-15} \text{ erg} \cdot \text{cm}^{-2} \cdot \text{sec}^{-1} \cdot \text{Å}^{-1}$. Since our spectra were taken with the smaller aperture $2.5'' \times 6''$, it is necessary to determine the correction for the aperture effect. We compared the continuum fluxes of NGC 5548 at 5100Å using spectra obtained in the same nights with our aperture $2.5'' \times 6''$ and with the aperture $5'' \times 7.5''$ of Peterson et al. (2002). The spectral observations during 13 different nights were used. The average correction for aperture effect is $\Delta F = F((5'' \times 7.5'') - F(2.5'' \times 6'')) = 0.35 \cdot 10^{-15} \text{ erg} \cdot \text{cm}^{-2} \cdot \text{sec}^{-1} \cdot \text{Å}^{-1}$. The host galaxy contribution at 5100Å with aperture $2.5'' \times 6''$ is $F(5100)_{\text{gal}} = (2.55 \pm 0.54) \cdot 10^{-15} \text{ erg} \cdot \text{cm}^{-2} \cdot \text{sec}^{-1} \cdot \text{Å}^{-1}$;

b) For the determination of the host galaxy contribu-

tion to the continuum flux of NGC 5548 at the wavelength 4250Å the spectrum of the normal E galaxy NGC 4339 was used. The spectral observations of NGC 4339 were taken with the 2.1 m telescope with the same aperture $2.5'' \times 6''$ and with the same spectral resolution ($\approx 8\text{Å}$) as the spectrum of NGC 5548 in the minimum activity state. After that we compared the spectra of NGC 4339 with the spectrum NGC 5548 in the minimum state (June 4, 2002). Such a comparison is justified because the central colors of the host galaxy NGC 5548 ($B-V \approx 0.9$; $V-I \approx 1.2$), are similar to the colors of an elliptical galaxy (Romanishin et al. 1995). We varied the contribution from NGC 4339 at 5100Å from 50% to 100% of that in the observed spectrum of the NGC 5548 and found, using a good subtraction of the absorption lines, that in the minimum activity of NGC 5548 the host galaxy contributes around 70% to the total continuum flux at 5100Å (see Figure 5). From Shapovalova et al. (2004) the observed flux at 5100Å in NGC 5548 for the minimum spectrum in aperture $2.5'' \times 6''$ is $F(5100) \approx 3.7 \cdot 10^{-15} \text{ erg} \cdot \text{cm}^{-2} \cdot \text{sec}^{-1} \cdot \text{Å}^{-1}$; and then the host galaxy of NGC 5548 flux is $F(5100) \approx (3.7 \cdot 0.7) \cdot 10^{-15} = 2.5 \cdot 10^{-15} \text{ erg} \cdot \text{cm}^{-2} \cdot \text{sec}^{-1} \cdot \text{Å}^{-1}$, that coincides with the value obtained by us, using the data from Romanishin et al. (1995).

We found that for NGC 4339 the fluxes ratio at 5100Å and 4250Å is $F(5100)/F(4250) = 1.45$. Supposing that the continuum of the host galaxy NGC 5548 is similar to that in NGC 4339 we found that the flux of host galaxy NGC 5548 at $\lambda 4250\text{Å}$ is $F(4250) = F(5100)/1.45 = (1.76 \pm 0.54) \cdot 10^{-15} \text{ erg} \cdot \text{cm}^{-2} \cdot \text{sec}^{-1} \cdot \text{Å}^{-1}$; Then we obtained the AGN-component continuum flux of the NGC 5548 at $\lambda 4250\text{Å}$ and 5100Å by subtraction of the continuum flux of the host galaxy. The measured fluxes only of the AGN-component are given in Table 1.

Note here that Peterson et al. (1995) showed that in the case of NGC 5548 the NLR has the same surface-brightness distribution as the PSF (i.e the NLR is point-like source $\sim 2''$), and that the point-source correction factor is always equal to one. Consequently, the broad-line/narrow-line flux ratio should be independent of the aperture and the seeing, at last for (slit) $\geq 2''$, that is the case in our sample of observations.

The total continuum flux ($F_t(\lambda)$) emitted at λ can be represented as a sum of the BLR (F_{BLR}), central source ($F_c(\lambda)$) and stellar continuum ($F_s(\lambda)$). As we noted above, the stellar continuum is subtracted and then:

$$F_t(\lambda, T) = F_c(\lambda, T_c) + F_{BLR}(\lambda, T_{BLR}). \quad (13)$$

Assuming that the optical continuum is originating far enough from the centre of an accretion disc, one can use the next relation for the central source of continuum (see Peterson 2004, Eq. 4.6 and corresponding discussion)

$$F_c(\lambda, T) \sim \text{const} \times \frac{T_c^{8/3}}{\lambda^{1/3}}, \quad (14)$$

If we neglect the contribution of the BLR continuum, the continuum flux ratio measured at λ_1 and λ_2 is

$$\frac{F_t(\lambda_1, T)}{F_t(\lambda_2, T)} \sim \left(\frac{\lambda_2}{\lambda_1}\right)^{1/3} = \text{const}. \quad (15)$$

There is no evidence that the continuum temperature is proportional to the BLR temperature, but one can assume that they are in correlation i.e. that $T_c \sim T_{BLR}$, therefore we will present the continuum intensity vs. the BLR temperatures.

In Figure 6, we present the AGN-component continuum flux variation as a function of the measured temperatures (at $\lambda 4250\text{\AA}$ in Figure 6a and at 5100\AA in Figure 6b) and the flux ratio variation (Figure 6c). As one can see from Figure 6a,b, the AGN-component continuum tends to be a linear function of the temperature. We found a high level of correlation between the continuum and temperature variability ($r = 0.85$). Also, we fitted the measured data with the continuum function as given by Eq. (14) and presented it with dashed line in Figure 6a,b, finding that Eq. (14) fits well the observed data.

Furthermore, as one can see from Figure 6c the AGN-component continuum intensity ratio at 4250 and 5100 \AA follows the expected function given by Eq. (15), i.e. remains constant as a function of the temperature. This also indicates the disc emission. But, here we should note that the temperature measured from the BLR fits very well the physical changes in the continuum.

This can be expected because of the following reason: whether illuminated by a variable hard X-ray source at the centre, or by some other mechanisms, the optical/UV continuum varies with the ionizing spectrum. Then, one can observe the continuum becoming "bluer" as it becomes brighter. This is consistent with an increase in the temperature of the thermal accretion disc as the central source (X-rays and the ionizing continuum emitting inner disc) brightens. The obtained high level of correlation between the AGN-component continuum and temperature, as well as of the ratio of the AGN-component continuum at different wavelengths and temperatures, support a dominant emission by an accretion disc in the BLR. As it was noted by Ulrich (2000) for the case of NGC 4151 the high correlation between X-ray emission (originated in an accretion disc) and temperature of BLR is expected. Here, we showed for the first time that this correlation exist in the optical part of the continuum.

On the other hand, the correlation obtained from our measurements may also be explained by the following: the emitting gas in the BLR becomes hotter when the central source brightness and the flux of incident photons increases. At the same time the sizes of the Stromgren zones increase in depth, increasing the optical depths in the Balmer lines. Their emitting efficiencies thus diminish with increasing incident flux, but the effect on $H\alpha$ is greater than that on $H\beta$, which is greater than the effect on $H\gamma$ (because $H\alpha$ optical depth remains greater than $H\beta$, etc., e.g. Ferland et al. 1979). In this case one can expect that the ratio of Balmer lines fluxes is a function of the continuum ratio measured in the blue and red part of the spectrum. To check it we presented the flux ratios of the continuum measured at 4250\AA and 5100\AA as a function of $H\alpha/H\beta$, $H\alpha/H\gamma$ and $H\alpha/H\delta$ flux ratios in Figure 7. As one can see from Figure 7, a slight tendency exists for the line ratios $F(H\alpha)/F(Hi)$ to be smaller

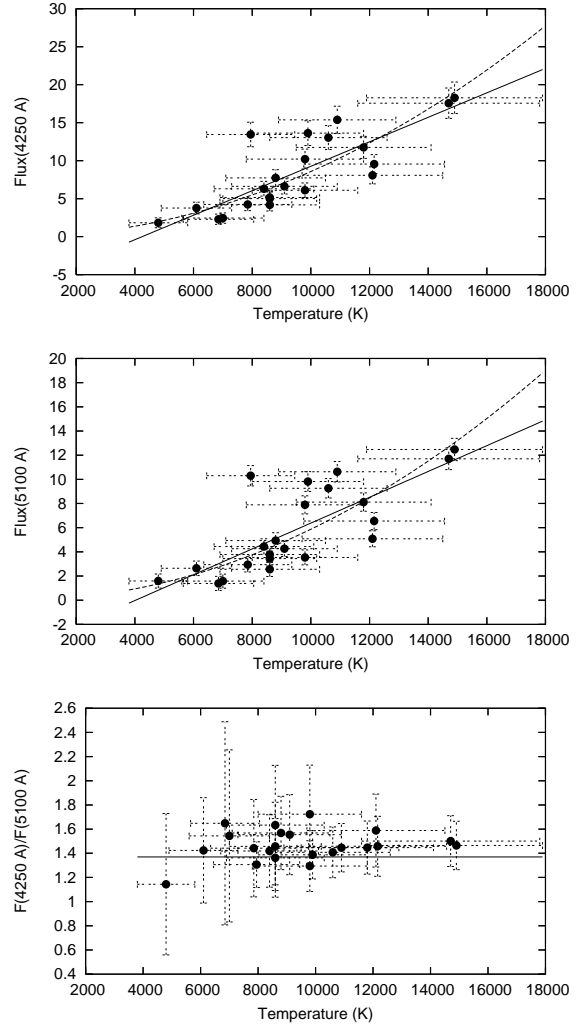


Fig. 6. The continuum flux measured at 4250 \AA and 5100 \AA as a function of the temperature measured with the BP (first two panels), and the ratio $I_C(4250)/I_C(5100)$ as a function of the temperature (bottom). The measured values are denoted with full circles. The assumed linear function and the function given by Eq. (14) are presented with full and dashed line, respectively (first two panels). In the 3rd panel the full line represents the best fit with Eq.(15).

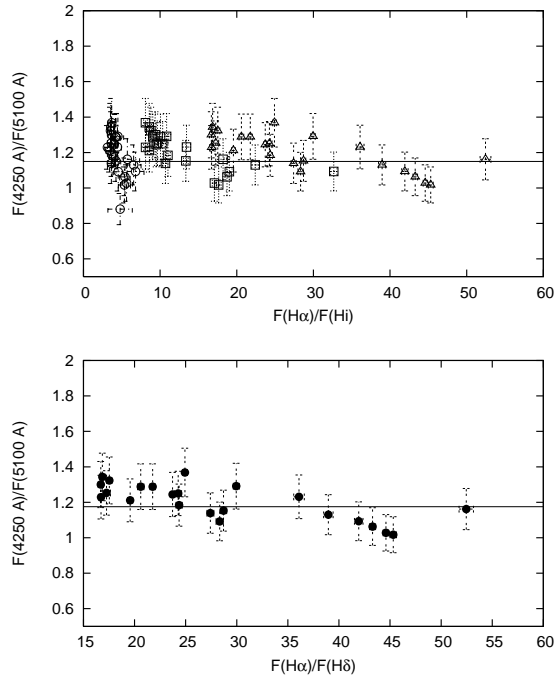


Fig. 7. The ratio of measured continuum flux as a function of the line flux ratios $H\alpha/H\beta$ (open circles), $H\alpha/H\gamma$ (open triangles), and $H\alpha/H\delta$ (open squares). In the bottom panel, the case for $H\alpha/H\delta$ flux ratio is presented separately.

when the continuum is bluer, but it is a very tiny effect. It indicates that we have the real correlation between the temperature and AGN-component continuum flux, that is presented in Figure 6.

6. Conclusions

By applying the BP method, as it was proposed by Popović (2003, 2006ab), to the broad Balmer lines of NGC 5548 observed from 1996 to 2004, we found that:

(i) it seems that the collisional processes play a significant role and that the distribution of the excited level population ($n > 2$) follows the Saha-Boltzman equation, and this should be taken into account when modeling the BLR of NGC 5548;

(ii) the BLR temperature was changed from 5000 K (in 2002) to 15000 K (in 1998). The average temperature is 10000 K, which is a value expected for the BLR. The maximum of the reached temperature corresponds to the region where the Balmer lines were the most intensive;

(iii) we found a correlation ($r = 0.85$) between the variation of optical AGN-component continuum and temperature; this is the first time that this correlation is confirmed, and it indicates the presence of an accretion disc in the BLR of NGC 5548 as it was earlier suggested by Shapovalova et al. (2004).

Acknowledgments

This work was supported by the Ministry of Science of Republic of Serbia through the project "Astrophysical Spectroscopy of Extragalactic Objects" (146002). Also, the work has been financed by INTAS (grant N96-0328), RFBR (grants N97-02-17625 N00-02-16272, 06-02-16843 and N03-02-17123), state program 'Astron' (Russia) and CONACYT research grant 39560-F and 54480 (Mexico). We would like to thank to the anonymous referee for very useful comments.

References

- Agekyan, T.A. 1972, *Osnovi teorii oshibok*, Nauka, Moscow.
- Baldwin J., Ferland G., Korista K., Verner D. 1995, *ApJ*, 455, 119
- Baldwin J., Ferland G., Korista K., Carswell R.F. Hamann F., Phillips M.M., Verner D., Wilkes B.J., Williams R.E. 1996, *ApJ*, 461, 664
- Bevington, P. R., Robinson, D. K. 2003, *Data reduction and error analysis for the physical sciences*, 3rd ed., Boston, MA: McGraw-Hill
- Burstein D., Heiles C. 1982, *AJ*, 87, 1165
- Crenshaw, D. M.; Kraemer, S. B. 2001, *ApJ*, 562, 29
- Crenshaw, D. M., Kraemer, S. B., Bruhweiler, F. C., Ruiz, J. R. 2001, *ApJ*, 555, 633
- Crenshaw D. M., Kraemer S.B., Gabel J.R., Schmitt H.R., Filippenko A.V., Ho L.C., Shields J.C., Turner T.J. 2004, *ApJ*, 612, 152
- Crenshaw D. M., Kraemer, S. B., Turner, T. J., Collier, S., Peterson, B. M. et al. 2002, *ApJ*, 566, 187
- Dumont A.-M., Collin-Souffrin S., Nazaroza L. 1998, *A&A*, 331, 11.
- Ferland G. J., Korista K. T., Verner D. A., Ferguson J. W., Kingdon J. B., Verner E. M. 1998, *PASP*, 110, 761.
- Ferland G. J., Netzer H., Shields G. A. 1979, *ApJ*, 232, 382
- Ferland G. J., Netzer H. 1979, *ApJ*, 229, 274
- Ferland G. J., Peterson B. M., Horne K., Welsh W. F., Nahar S. N. 1992, *ApJ*, 387, 95
- Gabel J. R. et al. 2005, *ApJ*, 631, 741
- Goad M. R., O'Brien P. T., Gondhalekar P. M. 1993, *MNRAS*, 263, 149
- Griem H. R. 1997, *Principles of Plasma Spectroscopy*, Cambridge University Press
- Ilić D. 2007, sent to *Serb. Astron. J.*
- Ilić D., Popović L.Č., Bon E., Mediavilla E. G., Chavushyan V. H. 2006, *MNRAS*, 371, 1610
- Ilić D., Popović L.Č., Ciroi S., La Mura G., Rafanelli P. 2007, sent to *ApJ*
- Kong M.-Z., Wu X.-B., Han J.-L., Mao Y.-F. 2004, *CJA&A*, 4, 518
- Konjević N. 1999, *Physics Reports*, 316, 339
- Korista K. T., Goad M. R. 2000, *ApJ*, 536, 284
- Korista K. T., Goad M. R. 2004, *ApJ*, 606, 749
- Krolik J. H. 1999, *Active Galactic Nuclei: From the Central Black Hole to the Galactic Environment* (Princeton: Princeton Univ. Press)
- Krolik J.H., Horne K., Kallman T.R., Malkan M.A., Edelson R.A., Kriss G.A. 1991, *ApJ*, 371, 541
- Kwan J. 1984, *ApJ*, 283, 70
- Kwan J., Krolik J. H. 1981, *ApJ*, 250, 478
- Laor A. 2006, *ApJ*, 643, 112

- Marziani P. M., Sulentic J. W., Dultzin-Hacyan D., Calvani M., Moles M. 1996, *ApJS*, 104, 37.
- Netzer H. 1975, *MNRAS*, 171, 395
- O'Brien P. T., Goad M. R., Gondhalekar P. M. 1994, *MNRAS*, 268, 845
- Osterbrock D. E. 1989, *Astrophysics of Gaseous Nebulae and Active Galactic Nuclei* (University Science Books, Sausalito, California)
- Peterson B. M. 2004, *An introduction to Active Galactic Nuclei*, Cambridge University Press
- Peterson B. M., Pogge R. W., Wanders I., Smith S. M., Romanishin, W. 1995, *PASP*, 107, 579
- Peterson B.M. et al. 2002, *ApJ*, 581, 197
- Popović L.Č. 2003, *ApJ*, 599, 140
- Popović L.Č. 2006a, *ApJ*, 650, 1217
- Popović L.Č. 2006b, *Serb. Astron. J.*, 173, 1
- Rees M. J., Netzer H., Ferland G. J. 1989, *ApJ*, 347, 640
- Romanishin, W., Balonek, T. J., Ciardullo, R., Miller, H. R., Peterson, B. M., Sadun, A. C., Stirpe, G. M., Takagishi, K., Taylor, B. W., Zitelli, V. 1995, *ApJ*, 455, 516
- Shakura N. I., Sunyaev R. A. 1973, *A&A*, 24, 337
- Shields J. C., Frelund G. J. 1993, *ApJ*, 402, 425
- Schlegel D. J., Finkbeiner D. P., Davis M. 1998, *ApJ*, 500, 525
- Shapovalova A. I. et al. 2004, *A&A*, 422, 925
- Stirpe G. M. 1990, *A&AS*, 85, 1049
- Stirpe G. M. 1991, *A&A*, 247, 3.
- Sulentic J. W., Marziani P., Dultzin-Hacyan D. 2000, *ARA&A*, 38, 521
- Ulrich M.-H. 2000, *A&AR*, 10, 135
- Vestergaard M., Peterson B. M. 2005, *ApJ*, 625, 688
- Vlasyuk V. V. 1993, *Bull. Spec. Astrophys. Ops.*, 36, 107